Korean J. Chem. Eng., **30**(12), 2228-2234 (2013)
DOI: 10.1007/s11814-013-0172-y

pISSN: 0256-1115
eISSN: 1975-7220

Role of microporosity and surface functionality of activated carbon in methylene blue dye removal from water

Mohammad Asadullah*,*,†, Mohammad Shajahan Kabir**, Mohammad Boshir Ahmed**, Nadiah Abdul Razak*, Nurul Suhada Abdur Rasid*, and Airin Aezzira***

*Faculty of Chemical Engineering, Universiti Teknologi Mara, 40450 Shah Alam, Selangor, Malaysia
**Department of Applied Chemistry and Chemical Engineering, University of Rajshahi, Rajshahi 6205, Bangladesh
(*Received 4 March 2013 • accepted 8 September 2013*)

Abstract−Activated carbons have been prepared from jute stick by both chemical and physical activation methods using zinc chloride and steam, respectively. They were characterized by evaluating surface area, iodine number, pore size distribution, and concentration of surface functional groups. The chemically activated carbon largely featured micropore structure, while the physically activated carbon mainly featured macropore structure. The specific surface area of chemically and physically activated carbons was 2,325 and 723 m^2/g, while the iodine number was 2,105 and 815 mg/g, respectively. The concentration of surface functional groups was determined by Boehm titration method, which suggested that different types of surface functional groups are randomly distributed on chemical activated carbons, while it is limited for physical activated carbon. The microporosity along with surface functional groups provided a unique property to chemically activated carbon to adsorb Methylene Blue dye to a large extent. The adsorption of dye was also affected by the adsorption parameters such as adsorption time, temperature and pH. Comparatively, higher temperature and pH significantly facilitated dye adsorption on chemically activated carbon.

Key words: Activated Carbon, Jute Stick, Chemical Activation, Methylene Blue, Adsorption

INTRODUCTION

Activated carbons (AC) possess high surface area with micropore and mesopore structures and are known as efficient adsorbents for gas and liquid. The increasing environmental concern significantly increased the applicability of AC for industrial pollutants separation. The effluents from industries such as textile, leather, paper, ink and cosmetics as well as the industries that produce dyes are severely contaminated with dyes, pigments, surfactants and many other toxic chemicals. These contaminated effluents ultimately go to the surface water reservoir. The dye-contaminated water even at a very low concentration is visible and aesthetically unacceptable. As most dyes are toxic and primarily contaminate surface water, the water biota is the primary victim of dye contamination, and long exposure of dyes in water often causes food chain contamination, resulting in adverse health effects. Hence, it is mandatory to reduce contaminant concentration in effluent below acceptable range before being released into the environment by utilizing proper treatment process. Due to technological advancement, numerous processes have been attempted to remove dyes and other contaminants from effluent in the last few decades. The most frequently used processes are adsorption [1-4], oxidation-ozonation [5], photocatalysis [6], biological treatment [7], coagulation-flocculation [8] and membrane separation [9]. Among these, adsorption is the most versatile and economic. Although the biological treatment for organic compounds removal from water is to some extent effective, the removal of organic refractory contaminants has proven to be very ineffective. Even if the contaminants are non reactive, the adsorbent can remove contaminants satisfactorily [10-12].

A number of adsorbents are used for dye removal including agricultural wastes, wood materials, industrial wastes and synthetic materials [1]. Activated carbons, which can be produced from agricultural wastes, are known to be very effective adsorbents for dye adsorption [13]. The unique adsorption property is developed on the AC surface due to the development of microporosity, large surface area (usually 500-3,000 m^2/g) and variable characteristics of surface chemistry [14,15]. These properties of AC can be regulated by regulating the preparation methods and their conditions as well as by selecting the precursor materials. A very selective AC can be prepared with a precise preparation method from a suitable precursor for a specific dye separation.

The adsorption of dye molecules onto the AC surface depends on the pore size distribution, surface functionality as well as the size and shape selectivity of the molecules to be adsorbed. For optimum adsorption, the molecular size of the adsorbate needs to be quite fitted to the pore size of the AC. The pore size of the AC is classified as micropore (<2 nm), mesopore (2-5 nm) and macropore (>5 nm) [16]. Both in the gas phase and liquid phase separations, the micro- and mesopores play a major role [17,18]. The macropore structure leads to the smaller surface area of AC as well as the multilayer adsorption is limited in macropore, which is attributed to the lower adsorption capacity. Therefore, the pore size and structure of AC need to be optimized for a specific separation.

The activated carbon from hard wood is especially used for gas separation and that from soft wood is used for solution phase separation. The chemical activation using H_3PO_4, $ZnCl_2$, KOH and K_2CO_3 is known to produce micropore and mesopore structure in AC [19]. However, the physical activation using steam often produces acti-

†To whom correspondence should be addressed.
E-mail: asadullah@salam.uitm.edu.my, asadullah8666@yahoo.com

vated carbon with macropore structure [20]. Activated carbons from the soft cellulosic precursors, especially from agricultural residues, are widely used for dye molecule separation from solution [1]. Phenol and many inorganic contaminants such as arsenic and mercury are also potentially environmental hazards and are separated using AC prepared from agricultural residues [21].

The presence of functional groups on the AC surface provides polarity, which in turn influences adsorption properties. IR spectroscopic studies indicated that during heat treatment at high temperature to produce AC, most of the reactive functional groups on the surface of biomass are released as H_2O, CO_2 and many other small molecules, leaving behind quinolic, etheric, phenolic and ketonic functional groups [22]. These oxygen-containing surface functional groups provide acidic as well as basic properties depending on the ring structures [23]. The extent of ring condensation during activation also has a role to play to form a wide basal surface of AC, which facilitates the accommodation of dye molecules in adsorption. Some studies showed that during steam activation of char at 700-900 °C the structural features of carbon drastically changed due to the condensation of smaller ring systems (3-5 fused rings) to larger ring systems (≥6 fused rings) [24]. The studies also showed that the reactivity of remaining char with oxygen drastically decreased with increasing the contact time of steam with char. However, since chemically activated carbon is often produced at around 500 °C, much lower than steam activation temperature, a significant number of functional groups are assumed to be retained on the surface.

The preparation, characterization and utilization of activated carbons for dye separation were the objectives of this study. Jute stick, which is an abundantly available agricultural residue in most Asian countries, was used as a precursor for activated carbon preparation by chemical and physical activation methods. Both of the activated carbons were characterized and utilized for methylene blue dye separation.

EXPERIMENTAL

1. Preparation of Feedstock

Jute stick of commonly cultivated varieties, *Corchorus capsularis*, in Asian countries was collected, washed with distilled water and dried at 105 °C for 12 h. The particle size of 1-2 mm was prepared by grinding and sieving of original jute stick. The moisture content of the dried jute stick was found to be approximately 4 wt%. The physical properties, proximate and ultimate analyses of jute sticks have been published elsewhere [25]. The proximate analysis exhibited 76-78 wt% volatile fraction, 21-23 wt% fixed carbon and 0.62 wt% ash. The ultimate analysis resulted in 49.79 wt% C, 6.02 wt% H, 41.37 wt% O, 0.19 wt% N, 0.05 wt% Cl and 0.05 wt% S.

Zinc chloride (99.0%, BDH Chemical Co.) was used as an activating agent. Iodine (99.5%), Sodium thiosulphate (99%), Potassium iodide (99.5%), Hydrochloric acid (35%), Potassium dichromate (99.9%) were purchased from Loba Chemicals Co., India. Commercial activated carbon (Laboratory Reagent, Thomas Baker Chemicals Ltd.) and Methylene Blue (99.9%, Aldrich) were used in this investigation.

2. Preparation of Activated Carbon

The preparation of activated carbon from jute stick by chemical activation using $ZnCl_2$ involved three steps: (1) socking of reagent solution by jute stick particles, (2) low temperature (200 °C) carbonization to produce char and (3) high temperature (500 °C) activation of char as optimized in previous work [22]. About 50 g of dried jute sticks was mixed with $ZnCl_2$ solution and kept for about 15 h at room temperature. The solution was completely socked by the solid mass. The $ZnCl_2$ to jute stick ratio was adjusted to 1 : 1. The wet solid was then transferred into a stainless steel reactor. The reactor configuration, published elsewhere [26], was 25 cm long with 5 cm internal diameter. The inside temperature of the reactor was controlled by a temperature controller through a thermocouple inserted into the reactor.

Before heating the reactor, nitrogen gas was purged for about 10 min at the rate of 200 mL/min to replace the air inside the reactor. Then the reactor was heated to 200 °C at the heating rate of 5 °C/min and was held for at least 15 min at this temperature, while the nitrogen gas was continued to flow. During this operation, the jute stick particles were carbonized and converted to sticky and black semi solid mass. The temperature was further increased to activation temperature (500 °C) at the heating rate of 5 °C/min and the activation was continued isothermally for about one hour. The final product was washed with deionized water. For washing, the solid product was mixed with deionized water in a beaker and stirred for 20 min at 60 °C and then the solid mass was separated by means of a vacuum filter. The process was repeated in order to remove $ZnCl_2$ almost completely. To detect the presence of $ZnCl_2$ in the spent water, 2/3 mL of it was taken in a test tube and a few drops of $AgNO_3$ solution were added into it. Appearance of a white precipitate indicated the presence of $ZnCl_2$. Therefore, the washing of the product was repeated until no existence of white precipitate was observed in the test tube. Finally, the AC sample was dried at 105 °C for 24 h and stored in a desiccator. The activated carbon prepared by chemical activation method was denoted as ACC.

From the total weight loss due to the activation of jute stick, the yield and activation burn-off were calculated using the following Eqs. (1) and (2), respectively:

$$Y(\%) = \frac{M}{M_o} \times 100 \quad (1)$$

$$Y'(\%) = \frac{M - M_o}{M_o} \times 100 \quad (2)$$

where Y and Y′ are yield of activated carbon and activation burn-off, respectively. M is mass of activated carbon obtained and M_o is initial mass of jute sticks in dry basis.

The activated carbon was also prepared by physical activation method using steam under optimum conditions as investigated in our previous work [27]. In this method, 50 g of jute stick was placed in a stainless steel reactor and was heated to 700 °C at the heating rate of 5 °C/min under the nitrogen gas flow rate of 200 mL/min. When the temperature reached 700 °C, steam was started to flow through the char bed into the reactor. The steam flow rate was 75 mg/min. For steam generation, the water was supplied by a peristaltic pump into the upper hot zone of the reactor, where the water was suddenly vaporized and mixed up with nitrogen gas and then passed through the char bed. When the steam contacted the char, a gasification reaction took place, producing CO and CO_2 and leaving behind the porous carbon structure. At the end of the process, the reactor

was allowed to cool to room temperature. Finally, the activated carbon was washed with 0.1 M HCl to remove ash and then washed with deionized water to remove residual acid. This activated carbon was denoted as ACS.

3. Characterization

The ACC and ACS were characterized in terms of specific surface area, iodine number, pore size distribution and surface chemistry. The surface area and pore size distribution were measured by nitrogen adsorption method at −196 °C using a Surface Area Analyzer (Model: AUTOSORB-1) to elucidate the microporosity of activated carbons. For nitrogen adsorption studies, the samples were degassed for 24 h at 50 °C to ensure complete evacuation of micropore. The iodine number was determined based on the Standard Test Method (ASTM D4607-94). To quantify the surface functional groups such as carboxylic, phenolic, lactonic and basic groups, Boehm titration was performed using $NaHCO_3$, $NaCO_3$, NaOH and HCl solutions for reacting with surface functional groups.

4. Dye Adsorption

Activated carbons, ACC and ACS were used for Methylene Blue dye adsorption from water. In each experiment 0.1 g of adsorbent was added into 50 mL dye solution in a conical flask. The flask was sealed with paraffin tape to avoid evaporation and shaken for a desired length of time in a thermostatic orbital shaker at 25 °C. After adsorption, the solution was filtered out and the concentration of the residual dye solution was measured using a Visible Spectrophotometer (ANA-75) at λ_{max} 626 nm. The same procedure was followed for a blank experiment to avoid any experimental error. The equilibrium adsorption of dye from different concentrations on ACC was measured to evaluate the Langmuir and Freundlich adsorption isotherm models. The amount of dye adsorbed, x/m was calculated and fitted to the following Langmuir Eq. (3) and Freundlich Eq. (4):

Langmuir isotherm:

$$\frac{C_e}{x/m} = \frac{1}{K_L \cdot x_m} + \frac{C_e}{x_m} \quad (3)$$

where C_e is the remaining dye concentration in the solution under equilibrium condition (mg/L), x/m is the total quantity of dye adsorbed per unit weight of ACC at equilibrium (mg/g), x_m is the maximum monolayer adsorption capacity (mg/g), and K_L is the Langmuir adsorption constant (L/mg) and it is related to the free energy of adsorption. The straight line was fitted to the points by the least square method, where the slope of the regression line is $1/x_m$ and the intercept is $1/K_L 1/x_m$

Freunlich isotherm:

$$\text{Log } x/m = \text{Log } K_F + 1/n \text{ Log } C_e \quad (4)$$

where K_F (mg/g) is the Freundlich adsorption constant, and 1/n is the measure of adsorption intensity, determining the favorable ($0.1 < 1/n < 0.5$) or unfavorable ($1/n > 2$) adsorption isotherm.

RESULTS AND DISCUSSION

1. Yield, Surface Area and Iodine Number of Activated Carbon

The activation burn-off, yield, specific surface area and iodine number of ACC and ACS are determined and tabulated in Table 1. The mass that decreased during activation is called activation burn-off. The yield was accounted for by subtracting the activation burn-off from the total mass of biomass and it was 45.0% for ACC and 13.5% for ACS. In the chemical activation, the bond cleavage initiated by the reaction of $ZnCl_2$ and the functional groups of jute sticks resulted in the evolution of small molecules such as H_2O, CH_3OH, HCHO, CH_3COOH and CO_2. These small products were released from the carbon matrix as vapors, leaving behind the skeletal structure of carbons. This reaction took place on the outer surface as well as in the micropore surface, so as to increase the number of pores as well as the size of pores. The total solid yield could be accounted to around 50.0% under optimum condition, which after washing and drying resulted in 45.0%. The reactions that occurred in the chemical activation process were influenced by activation temperature, and thus progressively increased the activation burn-off, resulting in reduced yield of ACC as we have observed in our previous work [22]. However, the BET surface area, which was created by the activation burn-off, increased only up to 500 °C. Further increase of temperature from 500 to 600 °C resulted in reduced surface area. The maximum BET surface area obtained was 2,325 m^2/g, which is much higher than (1,624 m^2/g) our recently produced activated carbon from jute stick activated using H_3PO_4 [28]. This is also much higher than (1,015-1,141 m^2/g) many activated carbons prepared from agricultural wastes using NaOH and $ZnCl_2$ as activating agents [29-31].

Table 1. Yield, activation burn-off, surface area and iodine number of activated carbons

Carbon sample	Temperature (°C)	Activation burn-off (wt%)	Yield (wt%)	S_{BET} (m^2/g)	Iodine number (mg/g)
ACC	500	55.0	45.0	2325	2105
ACS	700	86.5	13.5	723	815

For physical activation, the major part (around 70%) of the total burn-off occurred at the pyrolysis temperature at round 500 °C, while another 16.5% mass reduction occurred at activation temperature (700 °C). This huge burn-off resulted in very low yield (13.5%) of ACS as well as it was indicative of less pore density but bigger pore size, and thus the surface area was also very low (723 m^2/g). A further note revealed that the iodine number was much higher for ACC (2,105 mg/g) than that of ACS (815 mg/g), which is an indication of predominant micropore structure of ACC and macropore structure of ACS. The iodine value of ACC is superior to many reported results [32,33].

2. Pore Size Distribution

The pore size distribution has been analyzed by different methods like Barrett, Joyner & Halenda (BJH), Dubinin-Astakhov (DA) and Density functional theory (DFT)/Monte-Carlo pore volume distribution using N_2 adsorption isotherm under liquid nitrogen condition. Fig. 1 illustrates the BJH cumulative adsorption pore volume distribution in terms of pore diameter. BJH adsorption was counted above the relative pressure of 0.3 at which the spontaneous condensation of gas molecule in the cylindrical pores was predicted. As Fig. 1 shows, around 85% of total pore volume (1.21 mL/g) belongs to micropore (pore size <20 Å), while 10% and 5% of total pore volume belong to mesopore (pore size 20-50 Å) and macropore size (pore size >50 Å), respectively, for ACC. However, around 48%

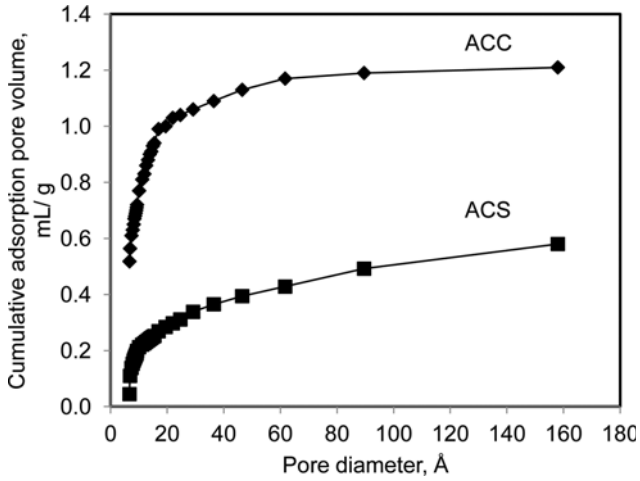

Fig. 1. Barrett, Joyner & Halenda (BJH) cumulative adsorption pore volume, (a) and cumulative adsorption surface area, (b).

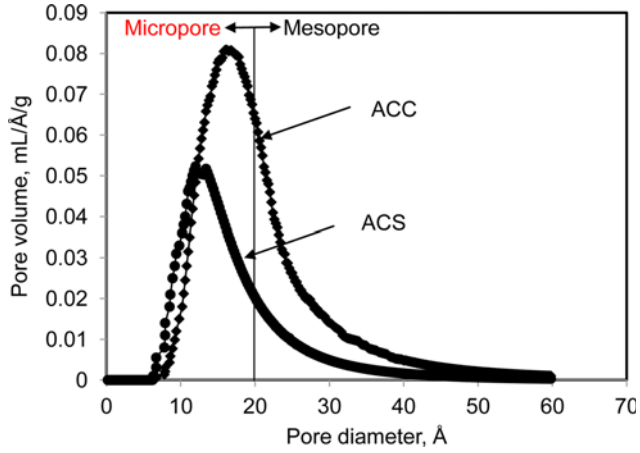

Fig. 2. Pore size distribution measured by Dubinin-Astakhov method for ACC and ACS.

of total pore volume (0.58 mL/g) belongs to micropore, while 21% and 31% of total pore volume belong to mesopore and macropore size, respectively, for ACS.

The DA method is often used to evaluate the micropore of activated carbons. In the DA equation, there are two variable parameters, (E_o) and n. E_o is denoted as the average adsorption energy, related to the pore diameter, and n is the width of the energy distribution, which is related to the pore size distribution. The values of n higher than 2 represents the homogeneous micropore structure of activated carbon, while lower than this value represents the heterogeneity of pores in meso- and macropore range. As Fig. 2 shows, the maxima of the micropore volume were much higher for ACC than that of ACS. It implies that the majority of the pore volume of ACC was related to the micropore structure compared to that of the ACS. It could be more clearly elucidated by the DFT/Monte-Carlo pore size distribution histogram as illustrated in Fig. 3. The figure shows that the sample ACC predominantly featured the micropore volume of 12-15 Å pore width, while it was almost one-fourth for ACS. The figure also indicates that a minor fraction of pore volume is related to macropore of ACC. Meanwhile, the pore volume of

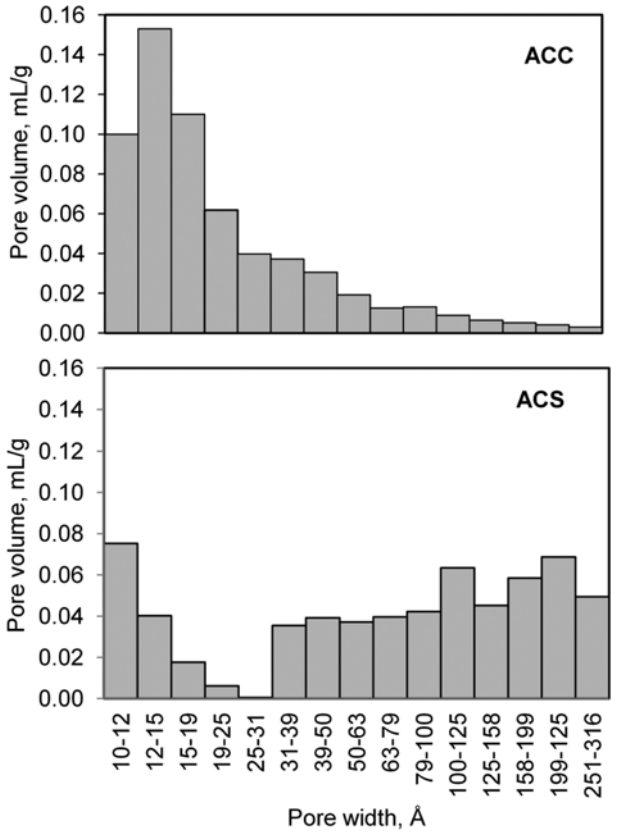

Fig. 3. Density functional theory (DFT)/monte-carlo pore volume histogram of ACC and ACS.

ACS is distributed in a wide range of macropore region. Therefore, it could be predicted that the micropore structure of ACC can adsorb methylene blue dye much more effectively than that of ACS, which is discussed in the subsequent sections.

3. Quantification of Surface Functional Groups

The existence of organic functional groups on the activated carbon surface provides surface polarity, which in turn contributes to adsorption properties. The number of exposed functional groups also depends on the surface area. Hence, the wide surface area with randomly distributed organic functional groups on activated carbon could presumably adsorb dye molecule more effectively. The functional groups on activated carbon were quantified by Boehm titration method and the results are summarized in Table 2. It can be seen that the major functional groups on ACC are carboxylic groups (1.61 mmol/g), followed by the phenolic (1.15 mmol/g), and lactonic groups (0.39 mmol/g), while these functional groups on ACS are 0.15, 0.13 and 0.04 mmol/g, respectively, much lower than ACC. The total acidic groups concentration on ACS is 3.15 mmol/g, which makes the surface highly acidic and it is presumed to be more effective to adsorb basic dyes like Methylene Blue. The acidity of the ACC surface is higher than reported results [34]. The basic characteristics of activated carbon surface generally evolve by the generation of basal plane, where the localized electrons of double bonds act as Lewis base. The basicity of ACC (1.45 mmol/g) is also higher than ACS (0.67 mmol/g).

4. Adsorption of Methylene Blue Dye (MB)

Methylene Blue is one of the representative basic dyes widely

Table 2. The concentration of surface functional groups of ACC and ACS

Activated carbon	Surface functional groups (mmol/g)				
	COOH	COO	>C-OH	Total acidic	Basic
ACC	1.61	0.39	1.15	3.15	1.45
ACS	0.15	0.04	0.13	0.32	0.67

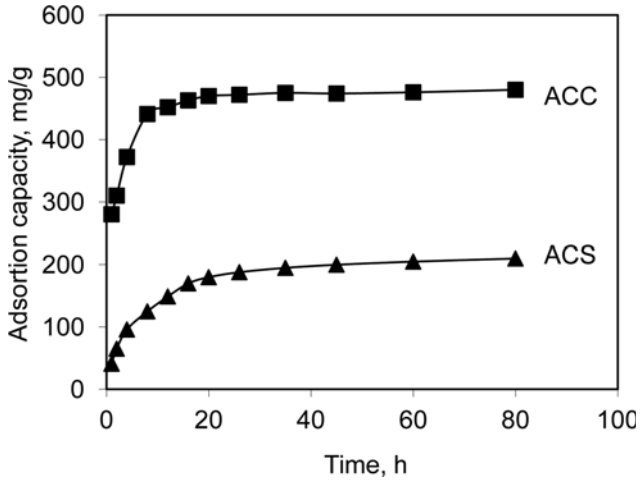

Fig. 4. Effect of contact time on methylene blue dye adsorption on ACC and ACS at 25 °C.

used in textile, leather and paper industries. It is also used as a model adsorbate to determine the solution phase adsorption capacity of carbon-based adsorbent. Fig. 4 illustrates the MB adsorption isotherm of two different adsorbents as a function of adsorption time at 30 °C. The equilibrium adsorption not only depends on adsorption time but also on the initial concentration of dye solution. The objective of this experiment was to determine the maximum MB adsorption capacity of both activated carbons in a specific adsorption time. Hence, the initial concentration of dye was comparatively higher (1,000 mg/L) than that of usual adsorption studies [35,36]. As can be seen in Fig. 4, ACS has very limited adsorption capacity compared to the ACC. The equilibrium adsorption of MB on ACS obtained was 210 mg/g even after 80 h, while it was 470 mg/g in 10 h for ACC. Compared to reported results, the MB adsorption on ACC is substantially higher [36-38]. From the characterization of ACC and ACS, the two adsorbents have completely different structural features with different surface functionality, which could feature the different adsorption capacity and mechanism. For ACC, most of the MB dye adsorbed on the micropore surface with stronger attraction force due to the presence of oxygen containing polar functional groups. It was also predicted that the micropores were completely filled with dye molecules irreversibly. Because of wide micropore surface of ACC with strong attraction force, the equilibrium adsorption was much faster than ACS. In contrast, the adsorption on the macropore surface with less functional groups of ACS resulted in weakly forced adsorption. The adsorbed MB molecules spontaneously desorbed, and thus it took longer time to attain equilibrium adsorption with much lower adsorption capacity compared to ACC.

Fig. 5 illustrates the effect of temperature on adsorption of MB

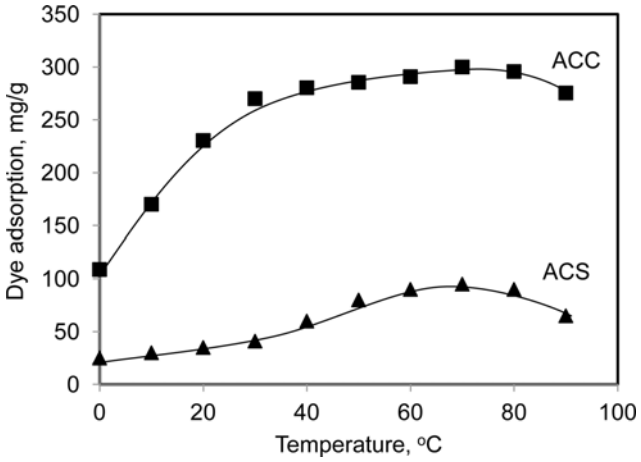

Fig. 5. Effect of temperature on methylene blue dye adsorption on ACC and ACS.

using ACC and ACS. Temperature can affect adsorption in two competitive ways. First, it can improve the diffusion rate of adsorbate molecules across the external boundary layer and internal pores of the adsorbent, so as to increase the adsorption rate. Second, it can weaken the force between adsorbate and adsorbent, so as to enhance the desorption rate. In MB dye adsorption on ACC, the amount of adsorption significantly increased with increasing temperature up to around 60 °C, while it was constant up to 80 °C. Further increase of temperature resulted in decreasing trend of adsorption. It could be predicted that the diffusion rate predominantly promoted the adsorption rate up to 60 °C and that was almost equal to desorption rate in between 60 and 80 °C. Above 80 °C, the desorption rate became prominent, and thus the adsorption decreased. The adsorption of MB molecules on ACS slightly increased with temperature up to 70 °C. This could be due to the less diffusion resistance for MB molecule to travel through macropore channel of ACS.

The pH is one of the most important factors that control the adsorption of dye onto adsorbent. From Boehm titration results, activated carbon surface possesses some oxygen containing functional groups. Those functional groups as well as the carbon in the aromatic ring system of activated carbon would be influenced by H^+ and OH^- ions at low and high pH, respectively. At low pH, where the H^+ ion was dominant in the solution, the species on the surface was assumed to be protonated, and thus the surface positive charge was assumed to be increased. During adsorption of MB, a positively charged dye, the surface charge partially repulsed the dye molecules; hence the dye uptake was lower at lower pH for both ACC and ACS as shown in Fig. 6. As pH increased, the dye uptake increased significantly up to pH 7. For ACC the isotherm remained plateau between pH 7 to pH 11; however, dye uptake jumped from 300 mg/g to 370 mg/g when pH changed from 11 to 13. It could be predicted that in the range of pH 7-11, the surface charge remained at zero point charge (pH_{ZPC}), where the adsorbent and adsorbate could utilize their inherent nature in adsorption. However, when OH^- ion became dominant in the solution at higher pH (>pH_{ZPC}), the adsorbent surface preferentially converted to negatively charged. Hence, the electrostatic attraction between positively charged dye molecules and negatively charged activated carbon surface significantly increased, which attributed to the sudden increase of dye adsorption

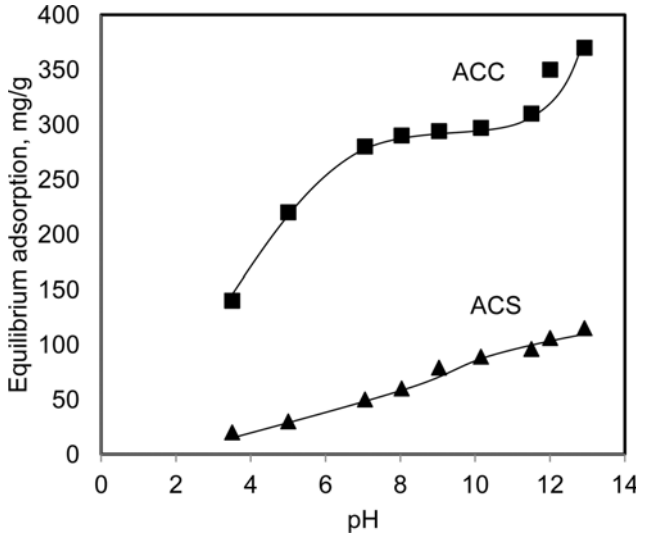

Fig. 6. Effect of pH on methylene blue dye adsorption at 30 °C on ACC and ACS.

Table 3. Langmuir and Freundlich isotherm parameters for methylene blue dye adsorption on ACC at 30 °C

Langmuir isotherm	K_L (L/mg)	R_L	R^2
	0.152	0.002	0.991
Freundlich isotherm	K_F (mg/g)	1/n	R^2
	67.0	0.306	0.936

by ACC.

5. Adsorption Isotherm

Adsorption of solute from solution was influenced by a number of parameters as discussed in the previous sections. Under suitable conditions, the maximum monolayer adsorption capacity is an important indicator of the quality of an adsorbent. This could be predicted by Langmuir and Freundlich adsorption isotherms, which are the most frequently used equations to characterize adsorbents, especially activated carbons. Eqs. (3) and (4) are the linear regressions of the Langmuir and Freundlich equations used for MB dye adsorption using ACC.

The isotherm parameters derived from the Langmuir and Freundlich adsorption isotherms are summarized in Table 3. The correlation coefficient (R^2 value) of the Langmuir isotherm is significantly higher than that of the Freundlich isotherm, implying the possible occurrence of monolayer adsorption. The result also suggests that the binding sites were homogeneously distributed on the activated carbon surface. The values of R_L derived from Langmuir isotherm were less than unity and 1/n derived from the Freundlich isotherm was between 0.1 to 0.5, suggesting that the adsorption processes was favorable under the experimental conditions and the data are quite similar to other works [29,30,35,36].

CONCLUSION

Nitrogen adsorption studies revealed that the micropore structure with wide surface area was developed in chemically activated carbon (ACC), while macropore structure with less surface area was developed in physically activated carbon (ACS). In addition, the surface functional groups of ACC are more significant than that of ACS. The micropore structure with organic functional groups on the surface favored dye adsorption more efficiently for ACC. At equilibrium, around 470 mg/g MB dye was adsorbed on ACC, while it was much lower for ACS (182 mg/g). The data of Methylene Blue dye adsorption from different initial concentrations of solution was better fitted to the Langmuir adsorption model compared to the Freundlich adsorption model, which suggested the possible maximum monolayer adsorption capacity. The separation factor R_L obtained was 0.002, between 0 and 1, which was a favorable value for ACC for efficient adsorption of Methylene Blue.

ACKNOWLEDGEMENTS

This research was financially supported by the Third World Academy of Sciences (TWAS) under the project no.: 07-033 LDC/CHE/AS-UNESCO FR: 3240144818 and The Ministry of Science and Information and Communication Technology (MOSICT 013A/06). The authors are grateful to the Faculty of Chemical Engineering, Universiti Teknologi Mara for providing the laboratory facilities to conduct a major part of this work.

REFERENCES

1. G. Crini, *Bioresour. Technol*., **97**, 1061 (2006).
2. G. Crini, F. Gimbert, C. Robert, B. Martel, O. Adam, N. Morin-Crini, F. D. Giorgi and P.-M. Badot, *J. Hazard. Mater*., **153**, 96 (2008).
3. G. Crini, H. N. Peindy, F. Gimbert and C. Robert, *Sep. Purif. Technol*., **53**, 97 (2007).
4. G. Crini and H. N. Peindy, *Dyes Pigm.*, **70**, 204 (2006).
5. M. F. Elahmadi, N. Bensalah and A. Gadri, *J. Hazard. Mater.*, **168**, 1163 (2009).
6. A. N. Soon and B. H. Hameed, *Desalination*, **269**, 1 (2011).
7. O. Türgay, G. Ersöz, S. Atalay, J. Forss and U. Welander, *Sep. Purif. Technol*., **79**, 26 (2011).
8. E. Guibal and J. Roussy, *React. Funct. Poly.*, **67**, 33 (2007).
9. Y. He, G. Li, H. Wang, J. Zhao, H. Su and Q. Huang, *J. Memb. Sci*., **321**, 183 (2008).
10. H. Lata, R. K. Gupta and V. K. Gar, *Chem. Eng. Commun*., **195**, 1185 (2008).
11. H. Lata, S. Mor, V. K. Garg and R. K. Gupta, *J. Hazard. Mater.*, **153**, 213 (2008).
12. D. W. Wang, F. Li, G. Q. Lu and H. M. Cheng, *Carbon*, **46**, 1593 (2008).
13. J. M. Dias, M. C. M. Alvim-Ferraz, M. F. Almeida, J. Rivera-Utrilla and M. Sanchez-Polo, *J. Environ. Manage*., **85**, 833 (2007).
14. M. Seredych, E. Deliyanni and T. J. Bandosz, *Fuel*, **89**, 1499 (2010).
15. A. Silvestre-Albero, J. Silvestre-Albero, A. Sepúlveda-Escribano and F. Rodríguez-Reinoso, *Micropor. Mesopor. Mater*., **120**, 62 (2009).
16. K. S. W. Sing, D. H. Everett, R. A. W. Haul, L. Moscou, R. A. Pierotti, J. Rouquerol and T. Siemieniewska, *Pure. Appl. Chem*., **57**, 603 (1985).
17. W. Zhao, V. Fierro, C. Zlotea, E. Aylon, M. T. Izquierdo, M. Latroche and A. Celzard, *Int. J. Hydrog. Energy*, **36**, 5431 (2011).
18. Z. L. K. Mui, W. H. Cheung, M. Valix and G. McKay, *J. Colloid*

Interface Sci., **347**, 290 (2010).
19. G. Skodras, I. Diamantopoulou, A. Zabaniotou, G. Stavropoulos and G. P. Sakellaropoulos, *Fuel Process. Technol*., **88**, 749 (2007).
20. M. Olivares-Marín, C. Fernández-González, A. Macías-García and V. Gómez-Serrano, *J. Anal. Appl. Pyrol*., **94**, 131 (2012).
21. D. Kalderis, D. Koutoulakis, P. Paraskeva, E. Diamadopoulos, E. Otal, J. O. del Valle and C. Fernandez-Pereira, *Chem. Eng. J*., **144**, 42 (2008).
22. M. Asadullah, M. Asaduzzaman, M. S. Kabir, M. G. Mostofa and T. Miyazawa, *J. Hazard. Mater*., **174**, 437 (2010).
23. H. P. Boehm, *Carbon*, **40**, 145 (2002).
24. D. M. Keown, J.-I. Hayashi and C.-Z. Li, *Fuel*, **87**, 1127 (2008).
25. M. Asadullah, T. Miyazawa, S.-I. Ito, K. Kunimori, M. Yamada and K. Tomishige, *Appl. Catal. A: Gen.*, **267**, 95 (2004).
26. M. Asadullah, M. A. Rahman, M. A. Motin and M. B. Sultan, *Ads. Sci. Technol*., **24**, 761 (2006).
27. M. Asadullah, M. A. Rahman, M. A. Motin and M. B. Sultan, *J. Surf. Sci. Technol*., **23**, 1 (2004).
28. M. Asadullah, I. Jahan, M. B. Ahmed, P. Adawiyah, N. H. Malek and M. S. Rahman, *J. Ind. Eng. Chem*., http:// dx.doi.org/10.1016/j.jiec.2013.06.019 (2013).
29. L. Lin, S.-R. Zhai, Z.-Y. Xiao, Y. Song, Q.-D. An and X.-W. Song, *Bioresour. Technol*., **136**, 437 (2013).
30. Y. Chen, S.-R. Zhai, N. Liu, Y. Song, Q.-D. An and X.-W. Song, *Bioresour. Technol*., **144**, 401 (2013).
31. A. Gundogdu, C. Duranb, H. B. Senturk, M. Soylak, M. Imamoglu and Y. Onal, *J. Anal. Appl. Pyrol*., http://dx.doi.org/10.1016/j.jaap.2013.07.008 (2013).
32. M. Loredo-Cancino, E. Soto-Regalado, F. J. Cerino-Córdova, R. B. García-Reyes, A. M. García-León and M. T. Garza-González, *J. Environ. Manage*., **125**, 117 (2013).
33. A. A. Ceyhan, Ö. Şahin, O. Baytar and C. Saka, *J. Anal. Appl. Pyrol.*, http://dx.doi.org/10.1016/j.jaap.2013.06.009 (available online, 2013).
34. H. Liu, J. Zhang, C. Zhang, N. Bao and C. Cheng, *Carbon*, **60**, 289 (2013).
35. A. L. Ahmad, M. M. Loh and J. A. Aziz, *Dyes Pigm.*, **75**, 263 (2007).
36. Ö. Gerçel, A. Özcan, A. S. Özcan and H. F. Gerçel, *Appl. Surf. Sci*., **253**, 4843 (2007).
37. K. Y. Foo and B. H. Hameed, *Chem. Eng. J*., **184**, 57 (2012).
38. S. K. Theydana and M. J. Ahmeda, *J. Anal. Appl. Pyrol*., **97**, 116 (2012).